AQUA
Water Infrastructure, Ecosystems and Society

Assessment of the minimal distance for placing household connections downstream of water distribution cross junctions

Rojacques Mompremier [a], Jersain Gómez-Núñez [a], Román Guadarrama-Pérez [b]
and Jorge Ramírez-Muñoz [a,*]

[a] Departamento de Energía, Universidad Autónoma Metropolitana-Azcapotzalco, Av. San Pablo Xalpa 180, Reynosa Tamaulipas, México City 02200, México
[b] TecNM: Academia de Ingeniería Química, Instituto Tecnológico Superior de El Mante, Ciudad Mante, C.P., 89930 Tamaulipas, México
*Corresponding author. E-mail: jrm@azc.uam.mx

RM, 0000-0003-3980-3321; JG-N, 0000-0002-9299-6401; RG-P, 0000-0002-4804-7874; RM-J, 0000-0003-1780-6185

ABSTRACT

This study investigates the solute (chlorine residual) mixing phenomena downstream of a cross junction, considering its critical role in house-hold connections. Experiments were conducted under turbulent flow conditions in a cross junction with two inlets at 90°, varying flow and chlorine concentration ratios at the inlets, i.e., simulating conditions commonly found in real water distribution systems. Results show that outlet chlorine concentrations primarily depend on the flow ratio at the inlets as well as on the inlet chlorine concentrations. Three-dimensional simulations were conducted to predict chlorine concentrations downstream of the cross junction. To evaluate the degree of downstream mixing, the percent coefficient of variation of tracer concentration (%CV) as a function of the axial position at different chlorine and flow ratios was computed from simulations. It was found that the flow ratio strongly affects it at downstream distances less than 50 pipe diameters, whereas the inlet chlorine concentration ratio has a weak effect. A novel correlation was derived as a function of flow ratio to ascertain the minimal distance for achieving the intended mixing level of %CV = 5 downstream of cross junctions. This correlation holds potential as a criterion for household connection location within water distribution networks for high-quality water delivery.

Key words: computational fluid dynamics, free chlorine concentration, household connections, incomplete mixing, water distribution systems

HIGHLIGHTS

- The study delves into chlorine residual mixing downstream of cross junctions.
- Experiments and simulations were performed to explore chlorine concentrations at the outlets.
- Simulations offering insights into distances for achieving intended mixing after junctions.
- A derived correlation identifies minimal mixing distance for household connections.
- Comprehending mixing at junctions aids public health and water management strategies.
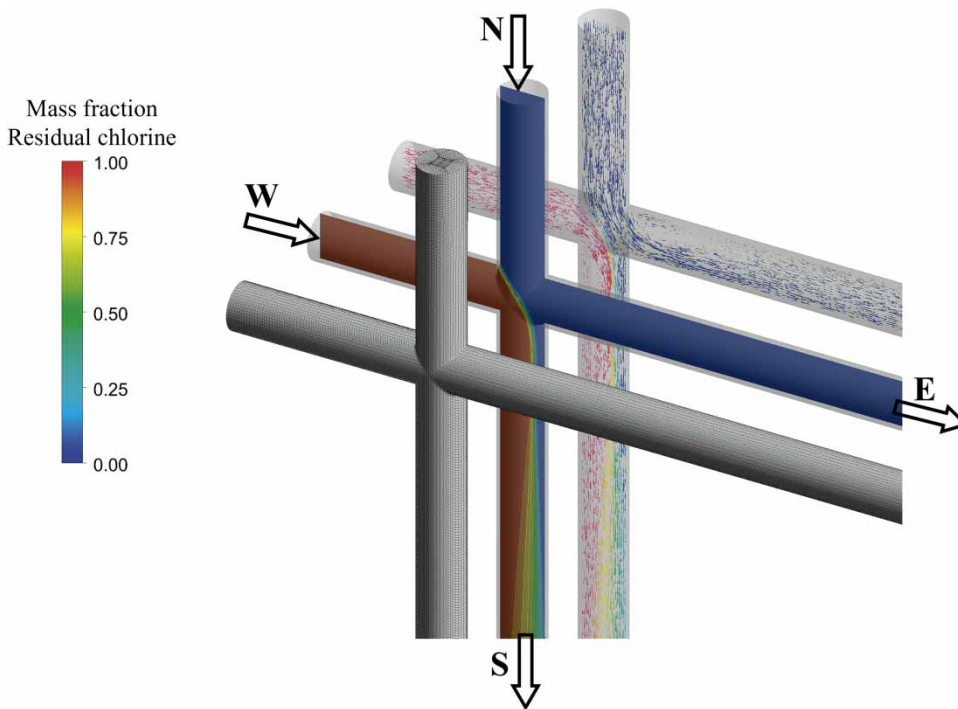
INTRODUCTION

Numerical modeling plays a critical role in predicting and managing water quality parameters, including residual chlorine, in distribution networks. Research on mixing phenomena is essential for understanding the distribution of water quality parameters such as disinfectants and contaminants throughout the network. Over the past decade, this phenomenon has gained considerable attention, especially in the water industry.

Numerous experimental and numerical studies using cross and T-junctions have been conducted due to their relevance in several applications, including particle trajectory monitoring and controlling the diffusion of solute concentrations exiting the junctions throughout the water distribution network (Choi *et al.* 2008; Romero-Gomez *et al.* 2008; Walker *et al.* 2010; Shao *et al.* 2014, 2019; Yu *et al.* 2014, 2016; Hernandez *et al.* 2021). Results of these studies show that incomplete mixing occurs at cross junctions when two or more fluid streams intersect. Additionally, the results indicate that mixing efficiency depends on several factors, including flow rates, Reynold numbers (Re), fluid properties, and junction geometry. These factors collectively influence the blending of different inflow streams, making their comprehension crucial for optimizing mixing at cross junctions. A few works considered most relevant in the context of this research will be discussed later.

Ho & O'Rear (2009) conducted experiments based on conductivity measurements of the two effluents to investigate the mixing behavior within individual pipe joints in a water distribution system. The experiment involved a single-node mixing setup with two entrances for water, a tracing material (used to visualize mixing), and the measurement of water conductivity at two outlets. The main objective was to understand how mixing occurs within pipe joints, specifically evaluating different joint configurations, pipe diameters, and flow rates. Their findings showed that the conductivity values at the two outlets were not equal. This suggests that the mixing process within the pipe joints was not perfect, with differences in concentration or composition between both outlets.

Ho & Khalsa (2007) developed models for a small-scale 3×3 pipe network to evaluate both complete and incomplete mixing models in pipe junctions of water distribution networks. Computational fluid dynamics (CFD) simulations demonstrated that accurate predictions of spatially variable tracer concentrations throughout the network could be achieved when compared to experimental data. Incomplete mixing within cross junctions was observed due to the bifurcation of incoming flows, with the extent of bifurcation and mixing largely dependent on the relative flow rates entering the cross junction.

In contrast, the first version of the EPANET model (Rossman 2000), assuming complete mixing within the junctions, produced uniform concentrations throughout the network, differing significantly from the spatially variable concentrations

observed in the experimental network. The EPANET model was modified after that to incorporate mixing correlations derived from previous single-joint experiments (Rossman et al. 2020). The results from this modified model accurately reflected incomplete mixing at the pipe junctions and aligned with the trends seen in the experimental data. Furthermore, additional CFD simulations demonstrated that networks consisting of T-junctions separated by at least several pipe diameters could be suitably modeled with complete-mixing assumptions.

Shao et al. (2019) studied experimentally the mixing phenomenon under laminar and transitional flow regimes, which is rarely reported. They reported that the average Reynolds number and the inflow Reynolds numbers ratio control the mixing degree at outlet pipe junctions. Austin et al. (2008) investigated the mixing phenomenon at cross junctions, exploring flow rates of 7.6 L/min or higher and at a wide range of Reynolds numbers within the turbulent regime. Their results indicated that the average dimensionless concentration and mass split through the outlets were 85 and 15%, respectively, suggesting incomplete mixing at the cross junction, unlike perfect mixing conditions where a mass split of 50% would be expected.

Solehati et al. (2014) conducted a numerical study to evaluate the mixing performance of a micro-channel T-junction with a wavy structure in comparison to a traditional straight micro-channel T-junction. The study yielded compelling results, demonstrating that the micro-channel with the wavy structure outperformed its conventional counterpart in terms of downstream mixing efficiency. The enhanced mixing observed in the micro-channel with the wavy structure was attributed to the presence of periodically reversed secondary flows generated by the curved wavy structure. These secondary flows created a chaotic flow within the micro-channel, significantly enhancing the mixing process.

Zughbi et al. (2003) carried out a numerical and experimental investigation of mixing in pipelines with side and opposed T-junction of different pipe diameters with cold water flowing in the main pipe and hot water through the tee. Their findings indicated that the downstream pipe length needed to achieve 95% mixing depends on the velocity ratio between the main pipe and the tee. Sun et al. (2020) conducted an experimental and numerical study on the mixing uniformity of water and saline solution injected as a tracer into the pipeline under turbulent conditions. They investigated the influence of pipe diameter, flow ratio, and Reynolds number on the mixing uniformity. The assessment of downstream uniformity was performed based on the coefficient of variation. Utilizing dimensional analysis, they derived an equation to predict the effective mixing length downstream from the tracer injection point within the proposed piping system.

Based on the previously discussed studies, it becomes evident that the water exiting a cross junction results from a combination of inlet flow rates, and often, incomplete mixing is observed with two inlets at 90°. In laboratory studies, cross junctions with short inlets and outlets have frequently been chosen, and therefore, most experiments have primarily focused on monitoring chlorine concentration variations at both outlets immediately after leaving the junction or until the pipe end. To our knowledge, no prior study has specifically examined the diffusion of chlorine concentration downstream from cross junctions.

Ongoing chlorine reactions with diverse organic or inorganic materials, including organic sediments, dissolved metals from corroded pipes, pipe materials, and microbial biofilms, within drinking water distribution pipes lead to chlorine decay (World Health Organization 2017). Consequently, chlorine concentrations at the inlet of cross junctions may exhibit fluctuations and decline below the minimum recommended levels at specific points within the distribution network, depending on the traveled path. On the other hand, it has been observed that flows with different concentrations in pipes (Zughbi et al. 2003; Ho & Khalsa 2007; Ho & O'Rear 2009; Sun et al. 2020) or channels (Solehati et al. 2014) need to travel a certain distance from the cross or T-junctions to achieve homogeneity. Therefore, in a real distribution network, household connections (carrying water from the public mains into homes) connected at any point downstream of cross junctions, where the effluents are not yet homogeneous, may carry inadequate chlorine concentrations. Nonetheless, there is a lack of reported data on chlorine concentration diffusion at points further downstream from cross junctions.

From the earlier discussion, the objective of this research is to determine the minimal distance at which household connections should be located to ensure the delivery of high-quality water. In order to fulfill the aim of this research, an experimental study was conducted to investigate the mixing phenomenon at a cross junction with two inlets at 90°, focusing on the interaction between water streams with different flow and chlorine concentration ratios at the inlets. Furthermore, CFD simulations were carried out to predict chlorine concentrations downstream of the cross junction, providing a detailed analysis of the distribution of chlorine concentration at various points across the conduit cross section. The statistical percent coefficient of variation (%CV) was used for a quantitative analysis of the degree of mixing, providing valuable insights into the homogeneity of the fluid within the pipe system after leaving the cross junction. Finally, a novel correlation was developed to determine the pipe length required to achieve the targeted mixing level of %CV = 5 downstream of cross junctions.

MATERIALS AND METHODS

Experimental setup and preparation

In order to achieve the objectives of this research, 10 experiments were first conducted in a laboratory network system. The experimental design consisted of an interconnecting piping system with two entrances (North and West) and two outlets (South and East). The pipe network was constructed with polyvinyl chloride (PVC) material with an inside diameter (d) of 32 mm. The system also featured a water tank (4.0 m³ capacity) and two storage tanks (each with a capacity of 0.6 m³). Four flow meters were placed at the entrances and exits of the intersections. These operate through a turbine aligned with the flow and report instantaneous flows on a digital display located on their upper part. Communication between the two parts occurs through sensors that interpret the rotation of the turbine (CZ300s model, Contazara S.A., Spain). Instantaneous flow values were displayed on the screen with an uncertainty of ± 1 L/h. Figure 1 (legend C) shows the exterior part, as well as a longitudinal section that allows observing the location of the measuring turbine.

A B&C Electronics CL7635 advanced chlorine controller was used to measure (measuring range of 0.1–20 mg/L) and control residual chlorine in the experiment. A data logger (El-USB-4, Lascar Electronics) was connected to each device to collect the data for their analysis. The chlorine meters were connected through hoses to nozzles located upstream and downstream of the intersections. Finally, an Evans 4HME200 centrifugal pump was used to move the fluid from the reservoir to the storage tanks.

Experimental procedure

The flow control valves were previously adjusted by partially opening them to achieve the desired flow rate for 10 scenarios with varying inflows, ranging from 0.75 to 4.50 L/s at the North inlet and 0.45 to 2.40 L/s at the West inlet. This study involved 10 scenarios that simulated different inflow rates as water enters the cross junctions. In this scenario, the flows joined the cross junction at 90° (from North and West) and exited at the South and East outlets. The primary objective of the experiments was to investigate the downstream mixing of incoming flows as they pass through the cross junction. The flow rate and chlorine concentration were set for 10 scenarios with varying inflows ranging from 0.75 to 4.50 L/s at the North inlet and 0.45 to 2.40 L/s at the West inlet. Considering that the majority of water distribution systems operate in the turbulent regime, the experiments were performed in this regime.

During the experimental runs, clean (tap) water from the reservoir was pumped to the elevated storage tanks with a 4HME200 centrifugal pump. Sodium hypochlorite solution was added to the West and North storage tanks, resulting in chlorine concentrations ranging from 0.06 to 0.9 mg/L at the North and 0.50 to 1.65 mg/L at the West inlet. The solutions
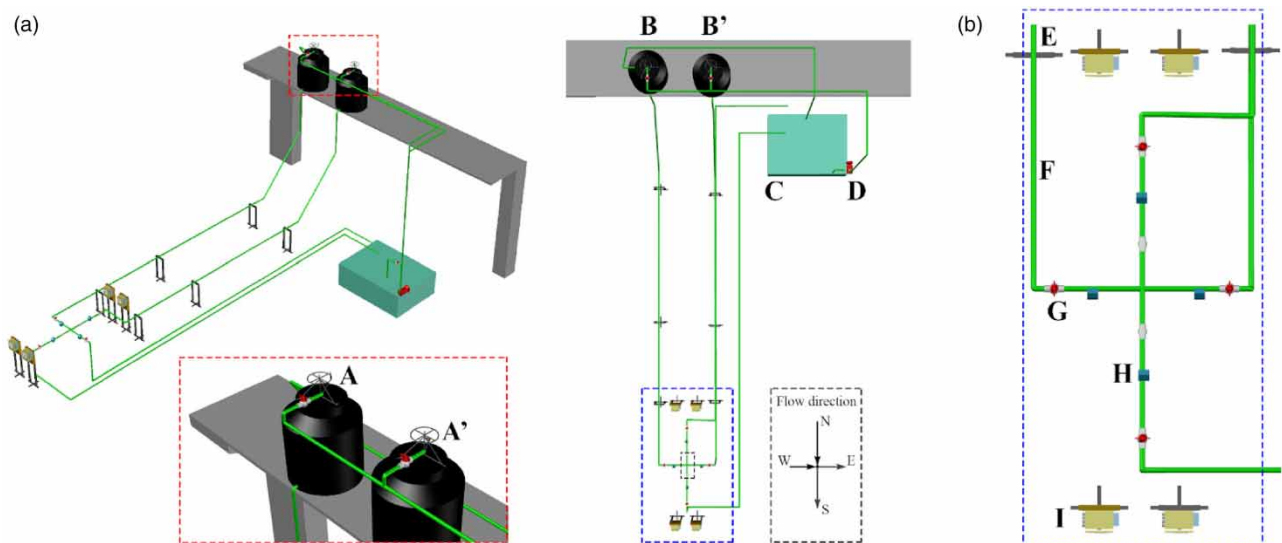

Figure 1 | Schematic diagram of the experimental water distribution network: (a) isometric view and (b) top view. A: West manual mixer; A': North manual mixer; B: West storage tank; B': North storage tank; C: water reservoir; D: centrifugal pump; E: metallic support; F: PVC pipe 32 mm; G: flow control valve; H: flow meter; I: chlorine meter.

in each tank were mixed with a hand mixer. All experiments were conducted at the standard room temperature of 20 ± 3 °C and ambient pressure.

The chlorine decay was neglected in this study since each experiment was extended for about 3 min. Instantaneous flow rates were measured using the flow meters at each inlet and outlet of the cross junctions. In all scenarios, the flows entering the North pipe, containing a lower chlorine concentration, were higher than those in the West inlet pipe. Free chlorine concentrations were also measured at each inlet and outlet. In order to corroborate the repeatability of experimental measurements, each experiment was repeated at least twice, and average results are reported. Predicting the exact flow magnitudes entering a cross junction in an actual water distribution network is nearly unfeasible; therefore, replicating the identical magnitudes is highly improbable. Thus, our scenarios established diverse relationships among inflow rates. The pivotal factor underlying this choice is that the scenarios were conducted under turbulent conditions, a consistent occurrence in real distribution networks. The description of the different scenarios in terms of flow rate and initial chlorine concentration is presented in Table 1.

Numerical flow modeling

In general, the fluid flow is described by the mass conservation and momentum laws; for an incompressible fluid, the mathematical formulation of these laws is expressed according to the following equations, respectively.

$$\frac{\partial u_i}{\partial x_i} = 0 \tag{1}$$

$$\frac{\partial u_i}{\partial t} + \frac{\partial}{\partial x_j}(u_i u_j) = -\frac{1}{\rho}\frac{\partial p}{\partial x_i} + \nu\frac{\partial^2 u_i}{\partial x_j \partial x_j} \tag{2}$$

where u_i and u_j are the velocity components in the i and j direction, ρ is the fluid density, p is the pressure, and ν is the kinematic viscosity. Although this set of equations is valid for any flow regime (namely, direct numerical simulations (DNS)), due to current computational limitations, it is not possible to solve it for the turbulent flow generated in the system examined in this work. An alternative to this problem is the use of the Reynolds decomposition in Equations (1) and (2), thus obtaining the well-known Reynolds-averaged Navier–Stokes (RANS) equations. In such a way, the continuity and momentum equations can be rewritten as (Pope 2000)

$$\frac{\partial \bar{u}_i}{\partial x_i} = 0 \tag{3}$$

$$\frac{\partial \bar{u}_i}{\partial t} + \frac{\partial}{\partial x_j}(\bar{u}_i \bar{u}_j) = -\frac{1}{\rho}\frac{\partial \bar{p}}{\partial x_i} + \nu\frac{\partial^2 \bar{u}_i}{\partial x_j \partial x_j} - \frac{\partial}{\partial x_j}(\overline{u_i' u_j'}) \tag{4}$$

Table 1 | Description of the different scenarios in terms of flow rate and chlorine concentration in the inflows

Scenario	North inlet (L/s)	West inlet (L/s)	North Cl$_2$ (mg/L)	West Cl$_2$ (mg/L)	Re (North)	Re (West)
1	0.75	0.45	0.60	1.00	29,800	17,900
2	0.96	0.51	0.61	1.25	38,200	20,300
3	1.36	0.80	0.90	1.35	54,100	31,800
4	1.36	0.84	0.06	0.50	54,100	33,400
5	1.44	0.88	0.15	0.51	57,300	35,000
6	1.90	1.00	0.21	0.81	75,600	39,800
7	2.00	1.50	0.71	1.39	79,600	59,700
8	2.25	1.20	0.50	1.40	89,500	47,700
9	3.40	2.00	0.30	0.70	135,000	79,600
10	4.50	2.40	0.90	1.65	179,000	95,500

In Equations (3) and (4), the $\bar{u}_i$, $\bar{u}_j$ and $u_i^{'}$, $u_j^{'}$ terms represent the mean and fluctuating velocity components, respectively. Furthermore, $\overline{u_i^{'} u_j^{'}}$ is the Reynold stresses tensor, which can be modeled according to the Boussinesq hypothesis as (Pope 2000)

$$- \rho \overline{u_i^{'} u_j^{'}} = \mu_t \left(\frac{\partial \bar{u}_i}{\partial x_j} + \frac{\partial \bar{u}_j}{\partial x_i} \right) - \frac{2}{3} \rho \kappa \delta_{ij} \tag{5}$$

In Equation (5), μ_t is the turbulent viscosity, κ is the turbulent kinetic energy, and δ_{ij} represents the Kronecker delta. In this work, μ_t is determined by using the standard κ-ε model as (Andersson $et\ al.$ 2011)

$$\mu_t = \rho C_\mu \frac{\kappa^2}{\varepsilon} \tag{6}$$

where C_μ is a model constant equal to 0.09, and ε represents the rate of dissipation. For an incompressible and isothermal flow, κ and ε are given by

$$\frac{\partial(\rho\kappa)}{\partial t} + \frac{\partial}{\partial x_j}(\rho\kappa\bar{u}_j) = \frac{\partial}{\partial x_j}\left[\left(\mu + \frac{\mu_t}{\sigma_k} \right) \frac{\partial\kappa}{\partial x_j} \right] + G_\kappa - \rho\varepsilon \tag{7}$$

$$\frac{\partial(\rho\varepsilon)}{\partial t} + \frac{\partial}{\partial x_j}(\rho\varepsilon\bar{u}_j) = \frac{\partial}{\partial x_j}\left[\left(\mu + \frac{\mu_t}{\sigma_\varepsilon} \right) \frac{\partial\varepsilon}{\partial x_j} \right] + C_{1\varepsilon}\frac{\varepsilon}{\kappa}G_\kappa - C_{2\varepsilon}\rho\frac{\varepsilon^2}{\kappa} \tag{8}$$

where G_κ represents the generation of turbulence kinetic energy due to the mean velocity gradients. The values for the σ_κ, σ_ε, $C_{1\varepsilon}$, and $C_{2\varepsilon}$ constants were 1.0, 1.3, 1.44, and 1.92, respectively. These values have been determined experimentally, including frequently encountered shear flows like boundary layers, mixing layers, and jets (Joshi $et\ al.$ 2011).

To model the variation in chlorine concentration along the pipe, it is necessary to couple the flow model with the species transport equation, which can be written, for isothermal conditions without chemical reaction, as

$$\frac{\partial}{\partial t}(\rho w_k) + \frac{\partial}{\partial x_j}(\rho u_j w_k) = -\frac{\partial}{\partial x_j}J_k \tag{9}$$

In Equation (9), w_k represents the local mass fraction of the kth species, and J_k is the diffusion flux of species k. In turbulent flow, the mass flux can be written as

$$J_k = -\left(\rho D_{k,m} + \frac{\mu_t}{\mathrm{Sc}_t} \right) \frac{\partial w_k}{\partial x_j} \tag{10}$$

The $D_{k,m}$ term in Equation (10) represents the mass diffusion coefficient for species k in the mixture, and Sc_t is the effective Schmidt number for the turbulent flow. In this work, the standard Sc_t value ($\mathrm{Sc}_t = 0.7$) included in Ansys-Fluent was used in simulations.

Computational mesh and numerical considerations

The experimental system's three-dimensional (3D) geometry and computational grid were generated in the Ansys© 17.1 Design Modeler and Meshing Modules, respectively. A top 3D view of the geometry and the computational grid is shown in Figure 2. The origin of the Cartesian coordinates was set at the center of the cross junction. From this origin, the computational domain was chosen to extend a length equivalent to 4.5 pipe diameters upstream of the inlets (North and West) and 61.125 pipe diameters downstream of the outlets (South and East). This simulation strategy allowed us to reduce the grid and the computational cost by around 46%. In addition, different volumes were built in the computational domain to avoid the formation of non-hexahedral elements in the near cross section. Hexahedral cells with a maximum cell skewness of 0.8 were used for discretization. The boundary between the different computational regions was conformal. To selectively refine the mesh in areas where the solution gradients are high and thus increase the accuracy of numerical predictions, an extra refinement strategy was implemented in the near-wall region using the inflation tool included in Ansys©-Meshing. From this,
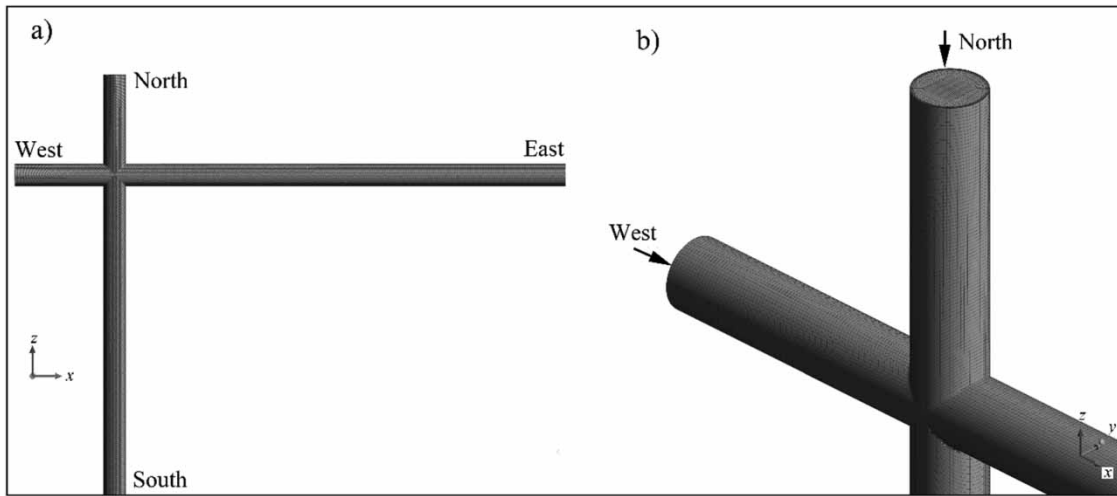
Figure 2 | The geometry and computational mesh near the cross junction: (a) top view and (b) isometric view.

capturing the existing velocity gradients near the pipe wall was possible. Details of the computational grid on the pipe surface in the North inlet can be appreciated in the isometric view of Figure 2.

In the study of fluid flow in pipe networks, friction losses are an important parameter to consider. According to Prandtl's theory, friction losses occur in a relatively thin region near the solid walls, referred to as the boundary layer (Bird *et al.* 2007), which is typically divided into three sublayers: viscous, buffer, and turbulent. In this context, to capture the influence of the flow in various regions of the boundary layer, the dimensionless parameter Y^+ is commonly employed in CFD simulations. This parameter relates the thickness of the boundary layer to the length of the computational cells close to the walls. According to Andersson *et al.* (2011), the values for Y^+ commonly used are $0 < Y^+ < 5$ (viscous sublayer), $5 < Y^+ < 30$ (transition sublayer), and $30 < Y^+ < 400$ (turbulent sublayer). In this work, to account for friction losses in the viscous sublayer, the length of the elements adjacent to the solid wall satisfies $Y^+ < 1$ for each examined computational mesh and all evaluated Reynolds numbers.

A fully developed turbulent velocity profile, as outlined by Bird *et al.* (2007), was implemented at both inlets as a boundary condition. This was coded in C language and compiled in Fluent to ensure the attainment of a fully developed state for both inlet flows before entering the cross junction. In the simulations, to differentiate that the currents from the North and the West enter with different concentrations of residual chlorine and to indicate that the West chlorine concentration is higher than the North one, a tracer mass fraction of one (1) was imposed as a boundary condition at the West inlet, while a tracer mass fraction of zero (0) was set at the North one. The concentrations of free chlorine at the East ($C_{Cl_2,E}$) and South ($C_{Cl_2,S}$) outlets were obtained from simulations, as follows (Bird *et al.* 2007):

$$Cl_{2,E} = w_{Cl_2,E}Cl_{2,W} + (1 - w_{Cl_2,E})Cl_{2,N} \tag{11}$$

$$Cl_{2,S} = w_{Cl_2,S}Cl_{2,W} + (1 - w_{Cl_2,S})Cl_{2,N} \tag{12}$$

in which $w_{Cl_2,E}$ and $w_{Cl_2,S}$ are, respectively, the area-weighted average tracer mass fraction in cross-sectional slices along the axial distance (East and South) extracted from simulations. Pressure outlet boundary conditions were imposed at the pipe outflows with a gauge pressure equal to zero (free discharge). In addition, non-slip boundary conditions were set on all wall surfaces.

The commercial CFD package Ansys©-Fluent 17.1 numerically simulates the present model with steady-state conditions and without gravitational effects. The standard κ-ε turbulence model with enhanced wall treatment for the near-wall condition was used for modeling the isothermal 3D turbulent flow. It has been reported that this model produces similar results for mixing in pipe cross junctions and T-junctions as the shear-stress transport (SST) turbulence model, with less computational effort (Walker *et al.* 2010; Santos-Violante *et al.* 2020). The standard pressure–velocity coupling, in conjunction

with a coupled scheme, was utilized. High-order spatial discretization was applied to the pressure, momentum equations, turbulent kinetic energy, turbulent dissipation rate, and species transport equations.

The species transport model incorporated in Ansys$^©$-Fluent was used to predict the solute concentrations at the outlets. The binary diffusion coefficient of the tracer species in the fluid was $D_{k,m} = 1.26 \times 10^{-9} \, m^2/s$, corresponding to chlorine's diffusion coefficient in water at 25 °C. In simulations, it was assumed that the tracer fluid (free chlorine in water) had the same viscosity (μ) and density as the main water flow, i.e., $\mu = 0.001$ Pas and $\rho = 998.3$ kg/m^3. Standard model constants predetermined in Fluent were used in all simulations. Each solution converged when all the scaled residuals remained constant, below 10^{-5}. No convergence problems were observed during simulations, i.e., the equation residuals always gradually decayed until the desired convergence was achieved.

RESULTS AND DISCUSSION

Experimental results

The focus of our study is the mixing of chlorine in pipelines downstream of cross junctions, which occurs over a duration of around 3 min. In contrast, the phenomenon of chlorine decay in water distribution systems extends over hours (Al-Jasser 2007; Romero-Gomez et al. 2008; Monteiro et al. 2014). Consequently, the decay of chlorine is considered non-significant in the context of our investigation and has been disregarded.

The experimental results of flow rates at inlets and outlets, as well as the mass balance of chlorine at inlets and outlets, are displayed in Figures 3 and 4. In all the scenarios analyzed, a relative error of less than 1% was detected when assessing the total flow balance and the chlorine mass flow. These results confirm the precise calibration of the equipment and instruments employed. In this study, the higher momentum from the North inlet led to some flow crossing over the junction into the opposite outlet (South). Therefore, the flow rate in the South is always higher than the inflow in the West.

Mesh independence analysis and numerical validations

Two critical aspects in CFD simulations that play a fundamental role in the reliability and precision of the numerical results are the computational mesh independence analysis and the validation of the numerical data. The mesh characteristics have a significant impact on the accuracy of the results at the expense of computational efficiency. Therefore, the mesh independence analysis ensures that the simulation converges toward a stable solution at a reasonable computational cost. On the other hand, the validation of the numerical data with experimental information ensures the reliability of the numerical results.

Table 2 shows the six computational meshes that were built in order to ensure that numerical results were independent of the mesh density. The number of cells between the coarsest and finest mesh varies between 250,880 and 3,043,784,
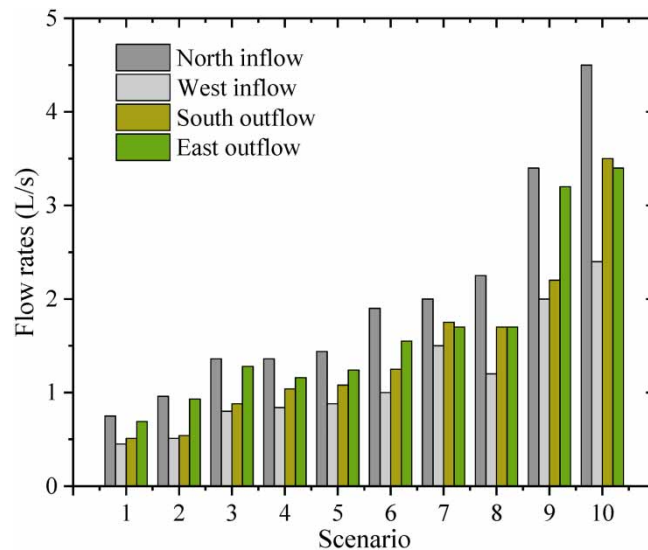

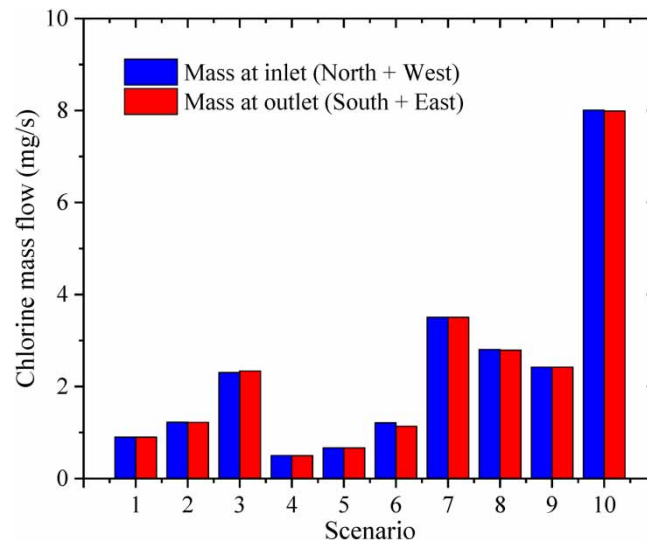**Figure 3** | Flow rates at inlets (North and West) and outlets (South and East).

Figure 4 | Mass balance of chlorine at inlets (North + West) and outlets (South + East).

Table 2 | Number of cells in the computational domain for the mesh independence analysis

Mesh	Number of elements
1	250,880
2	499,140
3	1,058,736
4	1,519,056
5	2,023,680
6	3,043,784

respectively. Numerical simulations for these six meshes were conducted at the highest Reynolds number (Re = 179,000) examined in this study.

The mesh independence analysis was carried out by increasing the number of elements in the radial, tangential, and axial direction of each pipe section in the same proportion and by comparing local values of tracer mass fraction as well as velocity magnitudes for two consecutive grid resolutions. If the difference between them was less than 3%, the numerical results based on the mesh with the lower number of cells were considered independent. Figure 5 shows profiles of tracer mass fraction and dimensionless velocity magnitude, v^* (normalized with the North inlet average velocity) along the centerline of the pipe (evaluated at pipe radius equal to zero) as a function of the dimensionless distance (l/L), where l is the axial distance from North, and L is the pipe length from North to South (or West to East). For both examined profiles, i.e., tracer mass fractions (Figure 5(a)) and dimensionless velocity magnitudes (Figure 5(b)), the mesh independence is attained with Mesh #4, and, for this mesh, the error with respect to the densest mesh values is less than 3%. Based on this, it was decided that Mesh #4, with 1,519,056 elements, could be considered independent and is the one used in further simulations.

A strategy commonly followed in validating CFD simulations is the calculation of hydrodynamic parameters from numerical results, and these are compared with experimental data. In this study, our measurements of chlorine concentration in both outlets (South and East) for the 10 scenarios analyzed were used to validate the computational results and are presented in Figure 6. The obtained maximum and average relative errors between the experimental and numerical data were 12 and 5%, respectively. Thus, it can be noted that the numerical predictions of chlorine concentration and the experimental measurements are in reasonably good agreement.

The initial chlorine dosage in the incoming flows turned out to be another important determinant of the chlorine concentration at the outlets. Furthermore, rather than achieving thorough mixing, flows tended to bifurcate (see Figure 7). As
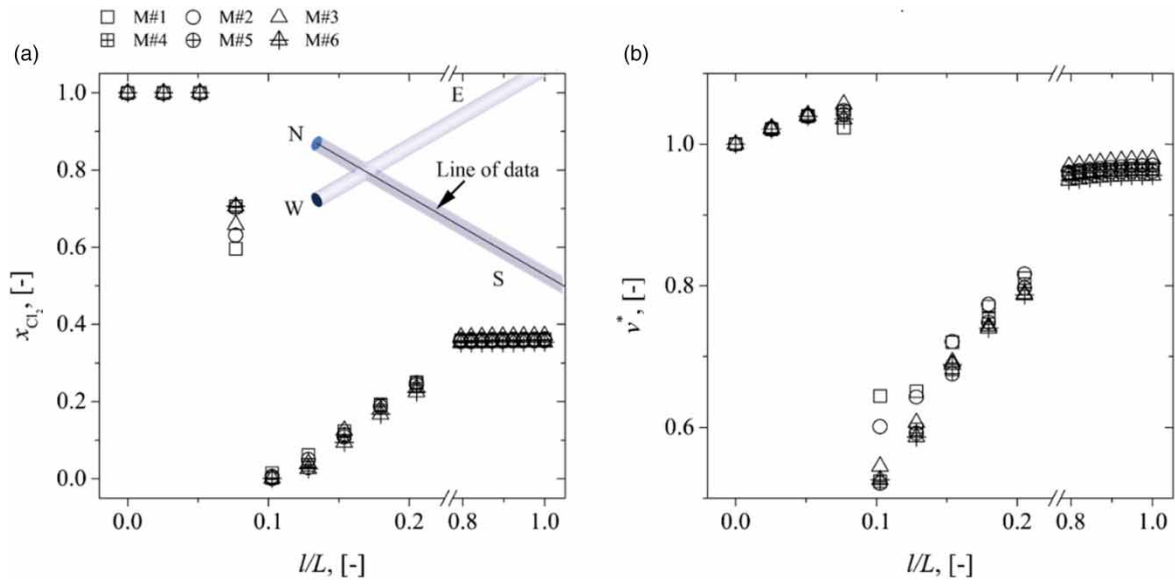
Figure 5 | Mesh independence analysis at the highest Re number examined in this study (Re = 179,000): (a) profiles of tracer mass fraction and (b) profiles of dimensionless velocity magnitude.
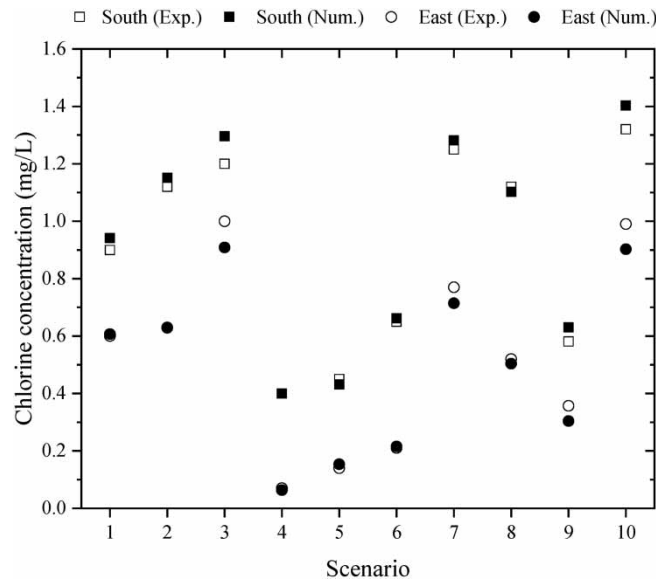

Figure 6 | Experimental and numerical chlorine concentrations at the outlets (South and East) for the 10 scenarios examined (see Table 1).

depicted in Figure 6, chlorine concentration varied between outlets in all scenarios due to this flow bifurcation. As observed, the primary factor influencing chlorine concentration at pipe junction outlets was the uneven flow rates within the cross junction. It is important to note that the concentration at the outlets also depends on the concentration at the inlets. Therefore, the greater the disparity between inlet concentrations, the more significant the variation observed in the outlets.

Throughout all the scenarios, consistently higher levels of chlorine concentrations were observed at the South outlet. This phenomenon can be attributed to the obstruction of flow at the West inlet caused by the incoming flow from the North, which had a lower flow rate. As a result, the effluent at the South outlet primarily consisted of water from the West inlet flow, leading to an elevated chlorine concentration. Chlorine concentrations ranged from 0.40 to 1.32 mg/L at the South outlet and from 0.07 to 1.00 mg/L at the East outlet. Ho & O'Rear (2009) made the same observation in their study where the clean water
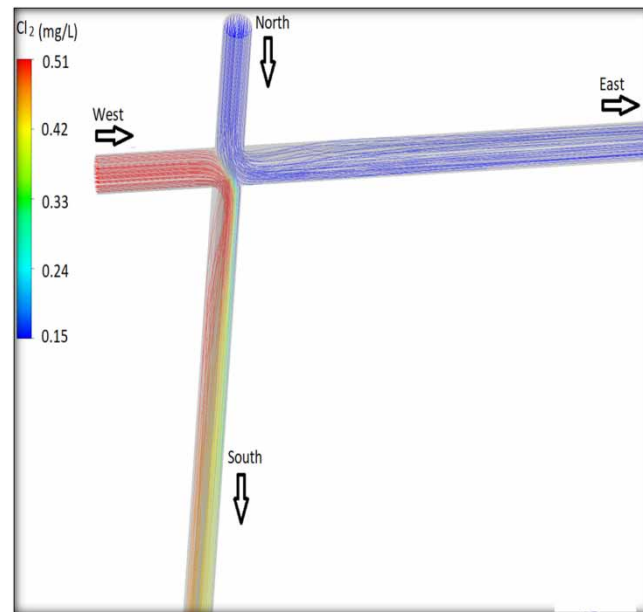
Figure 7 | Distribution of water flow lines and tracer contour concentrations in Scenario 5.

inlet flow rate exceeds the tracer inlet flow rate. They pointed out that the higher momentum of clean water flows across the junction diverts the incoming flow of the tracer water.

Determination of the degree of mixing downstream to the South

Numerical simulations were carried out to describe the mixing phenomenon at cross junctions to predict chlorine (Cl_2) concentration at the outlets. The distribution of water flow lines and tracer contour concentrations in the cross junction for Scenario 5 is shown in Figure 7. It is important to note that, in this figure, the red and blue color indicates the high and low concentrations of Cl_2 coming from the West and North inlets, respectively, which were different for each examined scenario. It can be seen here that the higher momentum from the North inlet resulted in a portion of the flow crossing over the junction and exiting through the South outlet, while all the flow coming from the West diverts toward the South. This causes a partial mixture of the two inflows to the South, while to the East, there is only the inflow coming from the North.

The contours of Cl_2 concentration in the wall–fluid interface and successive cross-sectional slices (each four-pipe diameters) along the axial distance to the South were extracted from the numerical simulations of Scenarios 6 and 7. These results are shown in Figure 8(a) and 8(b), at different inflow ratios in the North and West (Q_N/Q_W) and free chlorine concentration ratios in the North and West ($Cl_{2,N}/Cl_{2,W}$), respectively. An unmixed region or area is observed just after the fluid crosses the junction to the South, and the mixing uniformity improves substantially after a few downstream pipe diameters until a perfect mixing occurs. However, this uniformity of the fluid of the South outflow depends on the Q_N/Q_W ratio.

In Scenario 6 (Figure 8(a)), with a Q_N/Q_W ratio of 1.90 and a $Cl_{2,N}/Cl_{2,W}$ ratio of 0.26, a significant unmixing region was observed, indicated by the presence of distinct colors (blue, light blue, and green) immediately after the junction. Consequently, fluid uniformity remained compromised until the pipe end. Placing a household connection right after this cross junction could result in low-quality water delivery within the buildings, as achieving the intended homogeneity in mixing requires a specific downstream distance. Based on this example, the right placement for such a connection would be at the pipe's endpoint.

In Scenario 7 (Figure 8(b)), a lower value of Q_N/Q_W (1.33) was obtained. In this case, the incoming flow streams almost collide and exit through the adjacent pipe with some minor mixing. Consequently, a small unmixed area was observed, and the uniformity of the fluid was achieved closer to the junction compared to the previous test.

As shown in Figure 8(a) and 8(b), the area immediately downstream of the cross junction would carry an unmixed fluid with a lower disinfectant concentration (chlorine in the case of this study) since the fluid must travel some distance before achieving homogeneity.
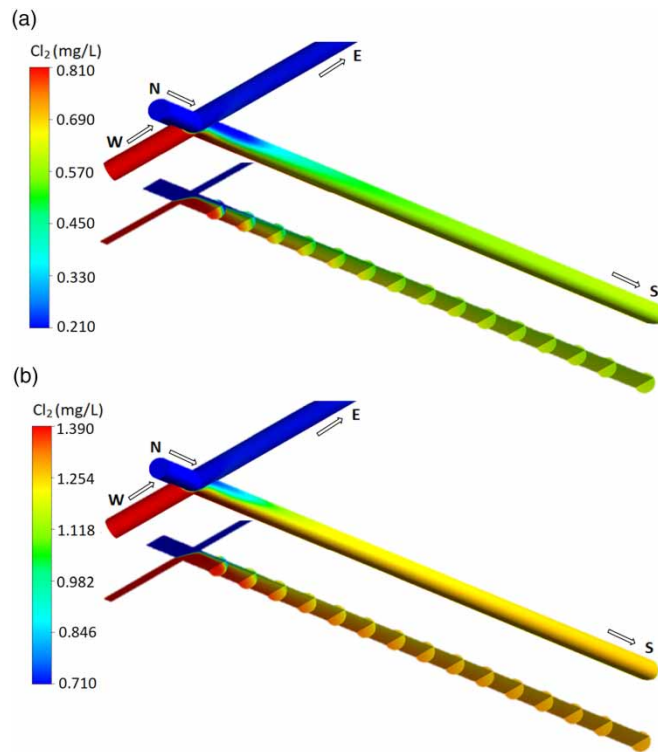
Figure 8 | Contours of Cl$_2$ concentration in the wall–fluid interface and successive cross-sectional slices of the fluid mixture along the South in (a) Scenario 6, $Q_N/Q_W = 1.90$ and Cl$_{2,N}$/Cl$_{2,W} = 0.26$; and (b) Scenario 7, $Q_N/Q_W = 1.33$ and Cl$_{2,N}$/Cl$_{2,W} = 0.51$.

Evaluation of the degree of mixing

A statistical method widely used to evaluate the degree of mixing in a flow circulating through pipes or static mixers is the coefficient of variation (Danckwerts 1952; Bakker *et al.* 2000; Liu *et al.* 2006; Sun *et al.* 2020; Jiang *et al.* 2021). This method consists of taking simultaneous samples of experimental or numerical data at various points over the conduit cross-section at fixed axial locations, which, when expressed as a percentage, is defined as follows:

$$\%CV = \frac{\sigma}{\bar{c}} \cdot 100 \tag{13}$$

where σ and $\bar{c}$ are, respectively, the standard deviation of the concentration, i.e.,

$$\sigma = \left(\frac{\sum\limits_{p=1}^{N} (c_p - \bar{c})^2}{N-1} \right)^{1/2} \tag{14}$$

and the average concentration of the mixture, given by

$$\bar{c} = \frac{\sum\limits_{p=1}^{N} c_p}{N} \tag{15}$$

Here, c_p is the local concentration of the tracer (free chlorine, in this case) at the pth mesh cell, and N is the number of evaluation mesh cells over the pipe cross-section. In this approach, the smaller the value of the coefficient of variation, the more homogeneous a tracer concentration is attained.

Figure 9 shows the %CV as a function of the dimensionless axial position at different Q_N/Q_W and Cl$_{2,N}$/Cl$_{2,W}$ ratios computed from numerical simulations for evaluating the mixture quality to the South. These values were extracted in the cross
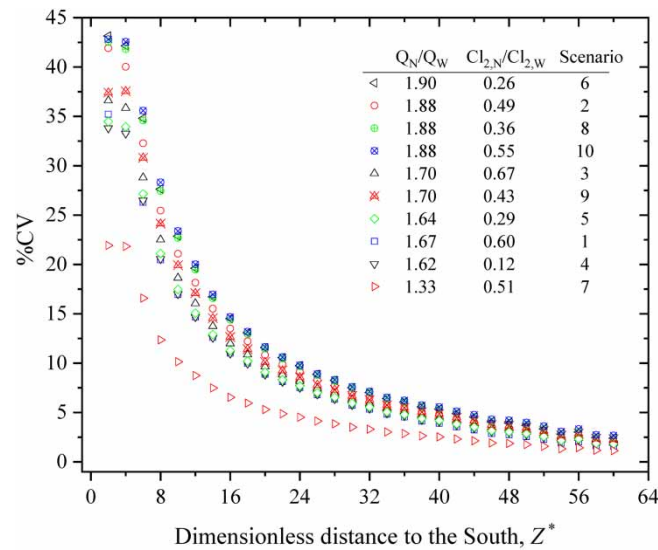
Figure 9 | Percentage of coefficient of variation (%CV) for different axial positions downstream to the South in 10 scenarios as shown in Table 1.

pipe section, each four-pipe diameters, as shown in Figure 8(a) and 8(b). Results show that under the turbulent flow conditions examined in this work, i.e., Re between 29,800 and 179,049, the concentration ratio, $Cl_{2,N}/Cl_{2,W}$, has little influence on the quality of the mixture downstream to the South. It can be seen qualitatively, in Figure 8(a) and 8(b), and quantitatively, in Figure 9, that, for distances less than approximately 50 pipe diameters, Q_N/Q_W has a strong effect on %CV. However, at greater distances, the %CV values for the 10 examined scenarios are very similar and fall below 3% and continue decreasing asymptotically. The results suggest that at a dimensionless distance downstream to the South ($Z^* = -z/d$) greater than 50 pipe diameters, the mixing degree is independent of both Q_N/Q_W and $Cl_{2,N}/Cl_{2,W}$. This might be attributed to the existing turbulence in the examined Reynolds numbers, which is adequate for accomplishing this mixing quality at this length of pipe (Etchells & Meyer 2003).

For much industrial blending of fluids, the accepted value used as a criterion for determining composition uniformity (i.e., a well-mixed system) is that %CV < 5 (Hobbs & Muzzio 1997; Bakker et al. 2000; Jiang et al. 2021). Based on this criterion, and by using the data of Figure 9, the following linear correlation for the dimensionless length of the pipe from the cross junction required to achieve %CV = 5 as a function of Q_N/Q_W and independent of $Cl_{2,N}/Cl_{2,W}$ was obtained:

$$Z^*_{\%CV=5} = 34.431 \cdot Q_N/Q_W - 22.08 \tag{16}$$

This equation was validated in the range $1.33 \leq Q_N/Q_W \leq 1.9$ and $17,900 \leq Re \leq 179,000$ (see Table 1), with $R^2 = 0.97$. However, for $1 \leq Q_N/Q_W < 1.33$, smaller initial values of %CV would be expected than the scenarios presented in Figure 9; therefore, the downstream pipe length required to achieve a coefficient of variation of 5% will be shorter. The majority of water distribution systems operate in a turbulent regime. Therefore, the obtained correlation (Equation (16)) can be reliably used under realistic operating conditions for $1 \leq Q_N/Q_W \leq 1.9$ and $17,900 \leq Re \leq 179,000$.

Due to the lack of data in the literature on the diffusion of chlorine concentration at locations further downstream from cross junctions, predictions from Equation (16) are compared with reported data on downstream mixing under turbulent conditions obtained from T-junctions by Zughbi et al. (2003) and Shao et al. (2014). Zughbi et al. (2003) observed that for a T-junction, the length of the pipe needed to achieve 95% mixing increases with the inlet velocity ratios, aligning with predictions from Equation (16). The term 'length of the pipe for achieving 95% mixing' in their study refers to the distance from the jet inlet to a point along the pipe where the measured quantity drops below 5% of the step input value. This concept is analogous to the coefficient of variation used in our study. When a side tee angle of 90 ° was utilized (refer to Figure (18) in Zughbi et al. 2003), which is more similar to our study involving a cross junction with two inlets at 90 °, they reported that, for the various examined pipe diameters (ranging from 1 to 16 in), 11 pipe diameters were needed to achieve 95%

mixing. For a double T-junction, simulation results reported by Shao *et al.* (2014) indicate that complete mixing of tracers occurs at a distance greater than 10 pipe diameters. Meanwhile, applying $Q_N/Q_W = 1$ in Equation (16), a distance of approximately 12.4 pipe diameters is required to achieve CV = 5%. Therefore, both reported results align well with those obtained in this study.

The degree of mixing of two fluids after leaving a cross junction is a crucial parameter in a water distribution system. It refers to how well two or more fluid streams mix after they intersect at a cross junction in a conduit. The level of mixing can significantly impact the quality and uniformity of the resulting fluid within the system.

Household connections represent an essential part of the water distribution network. Examining potential shifts in water quality parameters, particularly chlorine concentration, upon exiting the cross junction is significant for determining the right connection point along the main for the household. This analysis is crucial in preventing the delivery of water with undesirable or non-compliant chlorine concentrations.

CONCLUSIONS

The mixing phenomenon of incoming flows at pipe junctions plays a fundamental role in analyzing water quality within distribution networks, particularly in predicting solute transport. Experiments were carried out in a turbulent flow regime at a typical cross junction with two inlets (North and West) and two outlets (South and East). The present work explored a wide range of inflow rates, free chlorine concentrations, and Reynolds numbers, revealing incomplete solute mixing due to the bifurcation of the incoming flow. Additionally, a numerical study was performed using CFD, which yielded average relative errors between experimental and numerical results of chlorine concentrations at the outlets of 5%.

To evaluate the degree of mixing in junctions, a statistical method based on the coefficient of variation was applied. Simultaneous numerical data samples at various points across the conduit cross section, expressed as a percentage of the coefficient of variation, were collected. These data were gathered for different Q_N/Q_W and $Cl_{2,N}/Cl_{2,W}$ ratios, allowing us to assess mixture quality downstream. The accepted criterion for composition uniformity (indicating a well-mixed system) is %CV < 5.

A linear correlation was established to determine the dimensionless pipe length required to achieve %CV = 5 as a function of Q_N/Q_W. Our findings suggest that $Cl_{2,N}/Cl_{2,W}$ has minimal influence on downstream mixture quality, while Q_N/Q_W significantly affects it at distances less than 50 pipe diameters downstream.

Ensuring public health protection against contaminated water is of paramount importance. The results of this study enhance our understanding of how incoming flow rates and disinfectant ratios impact the mixing quality of effluents leaving junctions in water distribution systems. These findings can contribute to improving mathematical models for predicting disinfectant concentrations (chlorine) throughout the network and optimizing the placement of household connections downstream from cross junctions. In addition, the obtained correlation represents practical guidance for ensuring the delivery of safe and high-quality water to consumers.

DATA AVAILABILITY STATEMENT

All relevant data are included in the paper or its Supplementary Information.

CONFLICT OF INTEREST

The authors declare there is no conflict.

REFERENCES

Al-Jasser, A. O. 2007 Chlorine decay in drinking-water transmission and distribution systems: Pipe service age effect. *Water Research* **41** (2), 387–396.

Andersson, B., Andersson, R., Håkansson, L., Mortensen, M., Sudiyo, R. & Van Wachem, B. 2011 *Computational Fluid Dynamics for Engineers*. Cambridge University Press, Cambridge, UK.

Austin, R. G., Waanders, B. V. B., McKenna, S. & Choi, C. Y. 2008 Mixing at cross junctions in water distribution systems. II: Experimental study. *Journal of Water Resources Planning and Management* **134** (3), 295–302.

Bakker, A., LaRoche, R. D. & Marshall, E. M. 2000 Laminar flow in static mixers with helical elements. In: *The Online CFM Book*, Vol. 546. Available at: https://www.bakker.org/cfm/publications/cfmbook/lamstat.pdf.

Bird, R. B., Stewart, W. E. & Lightfoot, E. N. 2007 *Transport Phenomena*, 2nd edn. Wiley John Wiley & Sons, Inc., New York, NY.

Choi, C. Y., Shen, J. Y. & Austin, R. G. 2008 Development of a comprehensive solute mixing model (AZRED) for double-tee, cross, and wye junctions. In: *Water Distribution Systems Analysis 2008*, Kruger National Park, South Africa, pp. 1–10.

Danckwerts, P. V. 1952 The definition and measurement of some characteristics of mixtures. *Applied Scientific Research. Section A* **3**, 279–296.

Etchells III., A. W. & Meyer, C. F. 2003 Mixing in pipelines. In: *Handbook of Industrial Mixing: Science and Practice*, John Wiley & Sons, Inc.: Hoboken, NJ, pp. 391–477.

Hernández Cervantes, D., López-Jiménez, P. A., Arciniega Nevárez, J. A., Delgado Galván, X., Jiménez Magaña, M. R., Pérez-Sánchez, M. & Mora Rodríguez, J. D. J. 2021 Incomplete mixing model at cross junctions in Epanet by polynomial equations. *Water* **13** (4), 453.

Ho, C. K. & Khalsa, S. S. 2007 *A New Model for Solute Mixing in Pipe Junctions: Implementation of the Bulk Mixing Model in EPANET (No. SAND2007-6646P)*. Sandia National Lab. (SNL-NM), Albuquerque, NM, USA.

Ho, C. K. & O'Rear Jr., L. 2009 Evaluation of solute mixing in water distribution pipe junctions. *Journal American Water Works Association* **101** (9), 116–127.

Hobbs, D. M. & Muzzio, F. J. 1997 The Kenics static mixer: A three-dimensional chaotic flow. *Chemical Engineering Journal* **67** (3), 153–166.

Jiang, X., Yang, N. & Wang, R. 2021 Effect of aspect ratio on the mixing performance in the Kenics static mixer. *Processes* **9** (3), 464.

Joshi, J. B., Nere, N. K., Rane, C. V., Murthy, B. N., Mathpati, C. S., Patwardhan, A. W. & Ranade, V. V. 2011 CFD simulation of stirred tanks: Comparison of turbulence models. Part I: Radial flow impellers. *The Canadian Journal of Chemical Engineering* **89** (1), 23–82.

Liu, S., Hrymak, A. N. & Wood, P. E. 2006 Design modifications to SMX static mixer for improving mixing. *AICHE Journal* **52** (1), 150–157.

Monteiro, L., Figueiredo, D., Dias, S., Freitas, R., Covas, D., Menaia, J. & Coelho, S. T. 2014 Modeling of chlorine decay in drinking water supply systems using EPANET MSX. *Procedia Engineering* **70**, 1192–1200.

Pope, S. B. 2000 Turbulent flows, Cambridge University Press, Cambridge, UK.

Romero-Gomez, P., Choi, C. Y., van Bloemen Waanders, B. & McKenna, S. A. 2008 Transport phenomena at intersections of pressurized pipe systems. In: *Proceedings of the 8th Annual Water Distribution System Analysis Symposium*, Cincinnati, OH, USA.

Rossman, L. A. 2000 *EPANET 2 Users' Manual, EPA/600/R-00/057*. National Risk Management Research Laboratory, U.S. Environmental Protection Agency, Cincinnati, OH.

Rossman, L. A., Woo, H., Tryby, M., Shang, F., Janke, R. & Haxton, T. 2020 *EPANET 2.2 User's Manual*. Water Infrastructure Division, Center for Environmental Solutions and Emergency Response Office of Research and Development, U.S. Environmental Protection Agency, Cincinnati, OH. Available from: https://epanet22.readthedocs.io/en/latest/

Santos-Violante, H. A., Ramirez-Muñoz, J., Mompremier, R., Márquez-Baños, V. E., Guadarrama-Pérez, R. & Gómez-Núñez, J. 2020 CFD study of the effect of an internal device within a cross junction on mixing phenomenon. In: *2020 Virtual AICHE Annual Meeting Proceedings*. ISBN: 978-0-8169-1114-1.

Shao, Y., Yang, Y. J., Jiang, L., Yu, T. & Shen, C. 2014 Experimental testing and modeling analysis of solute mixing at water distribution pipe junctions. *Water Research* **56**, 133–147.

Shao, Y., Zhao, L., Yang, Y. J., Zhang, T. & Ye, M. 2019 Experimentally determined solute mixing under laminar and transitional flows at junctions in water distribution systems. *Advances in Civil Engineering* **2019**, 1–10.

Solehati, N., Bae, J. & Sasmito, A. P. 2014 Numerical investigation of mixing performance in microchannel T-junction with wavy structure. *Computers & Fluids* **96**, 10–19.

Sun, B., Lu, Y., Liu, Q., Fang, H., Zhang, C. & Zhang, J. 2020 Experimental and numerical analyses on mixing uniformity of water and saline in pipe flow. *Water* **12** (8), 2281.

Walker, C., Manera, A., Niceno, B., Simiano, M. & Prasser, H. M. 2010 Steady-state RANS-simulations of the mixing in a T-junction. *Nuclear Engineering and Design* **240** (9), 2107–2115.

World Health Organization 2017 *Principles and Practices of Drinking-Water Chlorination: A Guide to Strengthening Chlorination Practices in Small to Medium Sized Water Supplies*. World Health Organization, Regional Office for South-East Asia, New Delhi.

Yu, T. C., Shao, Y. & Shen, C. 2014 Mixing at cross joints with different pipe sizes in water distribution systems. *Journal of Water Resources Planning and Management* **140** (5), 658–665.

Yu, T., Qiu, H., Yang, J., Shao, Y. & Tao, L. 2016 Mixing at double-Tee junctions with unequal pipe sizes in water distribution systems. *Water Science and Technology: Water Supply* **16** (6), 1595–1602.

Zughbi, H. D., Khokhar, Z. H. & Sharma, R. N. 2003 Mixing in pipelines with side and opposed tees. *Industrial & Engineering Chemistry Research* **42** (21), 5333–5344.